

# Electron–phonon interaction in suspended highly doped silicon nanowires

A Tilke<sup>1</sup>, L Pescini, A Erbe<sup>2</sup>, H Lorenz and R H Blick

Center for NanoScience and Sektion Physik, Ludwig-Maximilians-Universität,  
Geschwister-Scholl-Platz 1, 80539 München, Germany

Received 25 March 2002, in final form 28 May 2002

Published 21 June 2002

Online at [stacks.iop.org/Nano/13/491](http://stacks.iop.org/Nano/13/491)

## Abstract

We have realized highly doped suspended silicon nanowires with lateral dimensions down to 20 nm for studying electron transport and dissipation phenomena in these wires. Random dopant fluctuations lead to the formation of multiple tunnel junctions, showing Coulomb blockade phenomena at low drain–source bias. In the finite-bias regime we observe relaxation of hot electrons via phonons. Melting of the wires then occurs at high bias values at an extremely large current density of the order of  $10^6$  A cm<sup>-2</sup>.

## 1. Introduction

One of the aims of semiconductor science and technology is the continuing size reduction of electronic systems such as transistors and memory elements. The fundamental problem of state-of-the-art integrated circuits is their large power consumption or in general the accumulation of heat due to energy dissipation in transistors and interconnects. As early as 1961 Rolf Landauer addressed the importance of dissipation for single-bit operations in transistors [1]. He also pointed out that the absolute limit for information exchange, which is the minimum amount of energy a single-bit operation requires, is given by  $k_B T \ln 2$ , which is  $3 \times 10^{-21}$  J at room temperature. This value is far below any complementary metal–oxide–semiconductor (CMOS) transistors' energy dissipation to date.

In order to address the physics of dissipation in the ultimate limit of single electrons interacting with phonon modes of their semiconductor host crystal, the most promising approach is to machine freely suspended nanobridges from doped semiconductor materials. These bridges allow us to study the electron relaxation via phonons [2] in detail by tailoring the phonon mode spectrum. The importance of the electron/phonon interaction in nanostructures was demonstrated by Fujisawa *et al* [3] and Qin *et al* [4] for non-suspended quantum dots in AlGaAs/GaAs heterostructures and theoretically modelled by Brandes and Kramer [5]. In early work on phonon waveguides, ballistic phonon transport through highly doped suspended semiconductor and metal wires with widths down to 100 nm at low temperatures was

reported [6]. Thermal properties of freely suspended GaAs nanostructures were then investigated by Tighe *et al* [7], while Beck *et al* [8] realized suspended two-dimensional electron gases (2DEGs) in AlGaAs devices for strain detection and Blick *et al* [9] recently presented first transport measurements on such 2DEGs and suspended quantum dots.

Similar efforts were undertaken in nanostructuring silicon-based materials: highly p-doped suspended silicon wires were investigated at room temperature by Fujii *et al* [10], while Pescini *et al* [11] built highly n-doped suspended silicon nanowires. Recently, an experiment by Schwab *et al* [12] revealed that in suspended silicon nanostructures the thermal conductance carried by phonons is quantized, as proposed earlier [13]. In transport measurements on metals such effects related to phonon dimensionality are usually masked, due to the large electronic contribution to the thermal conductance [14], but can also be found [15].

Here we present studies on energy dissipation of electrons in free-standing silicon nanowires, i.e. the electron energy relaxation via Brillouin zone edge phonon modes of these wires. We investigate electronic transport in highly n-doped suspended silicon nanowires in the sub-100 nm regime at temperatures ranging from 1.5 to 100 K. The advantage of this approach is the ability not only to control the electronic properties, but also to achieve thermal isolation from the underlying substrate. Due to random dopant fluctuations and segregation effects a potential landscape for electrons in the doped wires is created, leading to a serial arrangement of Coulomb islands, also termed multiple tunnel junctions (MTJs) [16, 17]. Due to these electron islands Coulomb blockade becomes visible in the *IV* characteristic of these structures at low source–drain bias. In the high-bias regime

<sup>1</sup> Present address: Infineon Technologies, Dresden 01099, Germany.

<sup>2</sup> Present address: Lucent Technologies, 600 Mountain Ave., Murray Hills, 07974 NJ, USA.

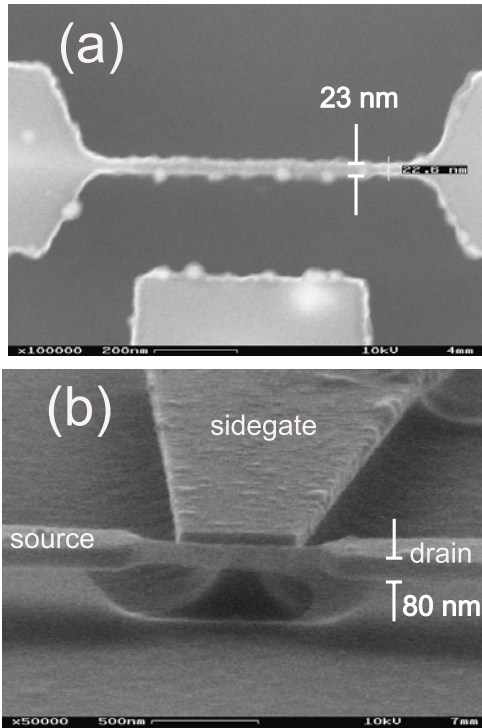


**Figure 1.** (a) Top view and (b) side view of the smallest suspended silicon nanowire fabricated with a width of 23 nm. The highly doped wire is clearly underetched; the sidegate allows us to tune the carrier density in the wire.

we observe a strong modulation of the wire conductance, being related to energy relaxation via Brillouin zone edge phonons. Finally, we demonstrate that the maximum current densities the nanowires can sustain are of the same order as those of conventional superconducting wires.

## 2. Experimental procedure

For sample preparation we use highly phosphorus-doped silicon on insulator (SOI) wafers with a silicon film thickness ranging from 80 to 150 nm and a 360 nm thick buried oxide layer (BOX). The doping concentration of the SOI film was chosen to be of the order of  $5 \times 10^{19} \text{ cm}^{-3}$  as determined by Hall measurements. In order to define suspended silicon nanowires we employ low-energy electron beam lithography with a two-layer PMMA electron beam resist in combination with a lift-off of a 50 nm thick evaporated Al film to create a hard masking for the subsequent dry etching. The masked silicon film is subsequently etched by  $\text{CF}_4$  reactive ion etching. Underetching of the BOX in buffered hydrofluoric acid (BHF) and drying of the samples in a critical point drier allow us to suspend the silicon nanobeams. Figure 1(a) shows a top view of the smallest structure: the minimum feature size achieved with this technique is 23 nm. Figure 1(b) shows the suspended nanostructure in a side view: the thickness of the wire is 80 nm; more details on the fabrication method are given in [11].

Finally, the samples are bonded and brought into the sample chamber of a variable-temperature insert (VTI) mounted in a helium bath cryostat, allowing a temperature variation from 1.5 up to 250 K. The measurement set-up

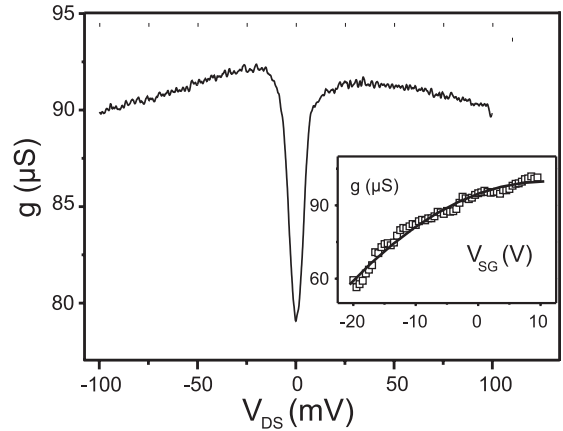


**Figure 2.** Conductance of a nanowire at low source–drain bias: at a temperature of 1.5 K a sharp resonance appears, resulting from MTJs in the wire. The inset shows the field effect at zero bias for this particular suspended nanowire measured at  $T = 2$  K with the conductance as a function of sidegate voltage  $V_{SG}$ . Due to the strong doping the wire is not fully depleted.

consists of a low-noise current preamplifier and a standard lock-in amplifier operated at a frequency of 130 Hz, applying a low ac voltage of  $v_{DS} = 100 \mu\text{V}$  across source and drain. Measurements at higher drain–source bias  $V_{DS}$  are performed by superimposing a dc offset on the ac sensing signal as discussed in detail elsewhere [18].

Figure 2 shows the conductance  $g = dI_D/dV_{DS}$  of a 50 nm wide, 150 nm thick and 500 nm long suspended nanowire in the low-bias regime as a function of the drain–source bias, with  $I_D$  being the drain current. A clear minimum of  $g$  is found around zero bias,  $V_{DS} = 0$  V, arising from the Coulomb blockade mechanism of the MTJs [19]. The charging energy  $E_C$  needed to add one more electron to the electron islands of the MTJ can be estimated if the temperature where the conductance dip disappears is known. Since the Coulomb blockade remains visible as long as the charging energy exceeds twice the thermal energy,  $E_C > 2k_B T$ , we can derive  $E_C \approx 4$  meV for the suspended nanowire. In our sample the wire conductance can effectively be tuned by an in-plane sidegate voltage  $V_{SG}$  (figure 1), as demonstrated in the inset of figure 2. As seen the resonance does not extend towards  $g = 0$ . Since the sidegate cannot decrease the conductance of the MTJs to values below  $e^2/h$  necessary to observe complete conductance suppression due to Coulomb blockade [20], the MTJs can only block several transport channels. In the non-linear  $I_D V_{DS}$  characteristic we find a conductance variation of 12% around  $V_{DS} = 0$ . According to [19], the number of electron islands  $N$  in the wire can be derived from the full width at half maximum of the conductance resonance  $V_{1/2} \cong 5.439 N k_B T / e$ . In this way we find  $N = 3$  [21].

In figure 3(a) the conductance  $g$  is measured up to high drain–source voltage at 1.5 K. In contrast to measurements on similar non-suspended structures [17], a strong modulation of  $g$  at high  $V_{DS}$  around  $\pm 0.5$  V can be found, which is almost independent of temperature as shown in the lower right inset of figure 3(a). This modulation cannot be explained by conventional Coulomb-blockade theory, but in terms of electron–phonon interaction. At low  $V_{DS}$  and low temperature, electron–phonon scattering in the suspended wire

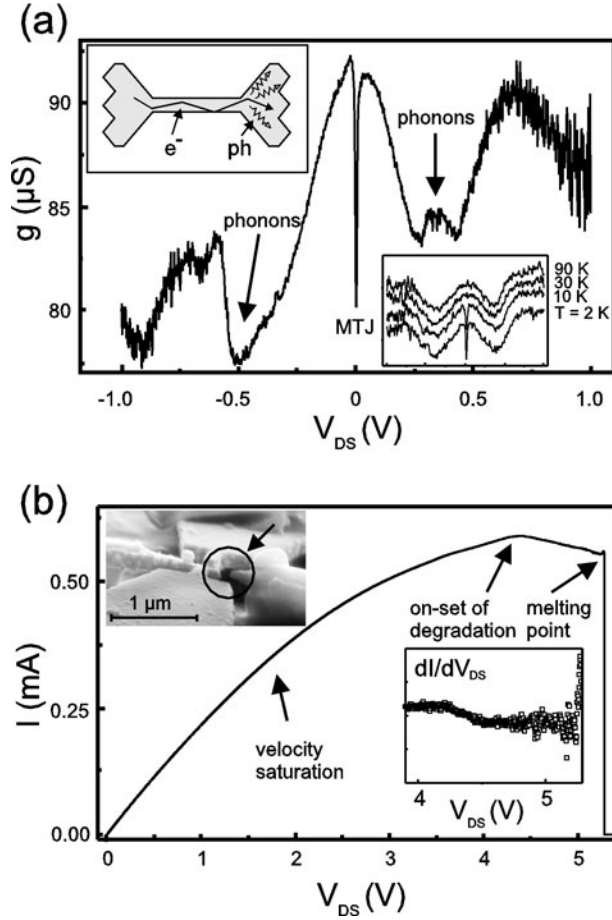


**Figure 3.** (a) Conductance of the nanowire at high  $V_{DS}$ : in the centre the MTJ resonance at 1.5 K is seen. Around  $\pm 0.5$  V we find a structure indicating electron relaxation via phonons at the Brillouin zone edge. The lower right inset shows the insensitivity of the phonon relaxation peaks up to 90 K, which supports the estimation of a wire temperature of about 600 K. The upper left inset schematically illustrates the assumed mechanism of electron thermalization occurring in the clamping points. (b) Maximum sustainable current through a  $100 \times 150$  nm<sup>2</sup> thin suspended nanowire. The nonlinearity at voltages below 4 V indicates velocity saturation of the hot electrons. The inset on the right shows the conductance close to the melting point. The left inset is the electron-beam micrograph of a similar device after melting: the edgewise break point is marked by the circle.

is strongly altered due to the reduced phonon density of states in the suspended wire. Electron thermalization occurs in the clamping points—as depicted in the upper left inset in figure 3(a)—where the phonon density of states changes from two to three dimensions.

In order to find the maximum amount of energy dissipated in the suspended nanowires the current is continuously increased. In figure 3(b) melting of a  $100 \times 150$  nm<sup>2</sup> wire at a bath temperature of 2 K is recorded. Prior to melting, seen in the jump of the current, the wire continually degrades (right inset of figure 3(b)). The maximum current density before the melting of this suspended beam is found to be  $4 \times 10^6$  A cm<sup>-2</sup>, which is comparable to current densities in conventional superconductors [22] and is only exceeded by nanotubes [23]. Melting finally occurs at the clamping points where the electrons find multiple phonon relaxation channels.

The upper left inset of figure 3(b) shows a melted nanowire recorded with an electron beam microscope.

In the low-bias regime only acoustic phonons can be excited while in the high-bias regime Brillouin zone phonons can also interact with the electrons. The observed conductance modulation is therefore likely to be the result of emission of zone-boundary phonons by high-energy electrons, as explained in detail by Yao *et al* [23]. Electrons scatter inelastically with phonons with a relaxation time  $\tau_{e-ph}$  causing dissipative heating of the wire. The heat input has an energy density of  $u_J(T) = \rho j^2 \tau_{e-ph}$ , where  $\rho$  is the specific resistance of the wire and  $j$  the current density [14].

Although for crystals of reduced dimensions there might be no sharp melting point [24], we are using the Debye model [25] and the melting point found in figure 3(b) to estimate  $\tau_{e-ph}$ . Since the electron–phonon scattering rate determines the rate of heat flow out of the electron gas, it is possible to compare the thermal energy stored in the wire at a given temperature  $T$ ,  $U_{ph}(T)$ , with the energy  $U_J(T)$  provided by the ohmic losses during the time  $\tau_{e-ph}(T)$ . In the limit  $T \gg \Theta$ , with  $\Theta = 640$  K the Debye temperature of silicon, the heat capacity  $C_V$  approaches the classical value  $3Nk_B$ , where  $N$  is the number of atoms in the suspended nano-crystal (here we consider a volume of  $100 \times 150 \times 1500$  nm<sup>3</sup> and an atomic density of  $5 \times 10^{28}$  m<sup>-3</sup>). Therefore, with a melting point for bulk silicon of 1680 K [26], the total phonon energy is found to be  $U_{ph}(T) = U_{ph}(1680 \text{ K}) = C_V T \approx 0.78 \times 10^{-10}$  J. The energy dissipated by Joule heating during the time  $\tau_{e-ph}$  is given by  $U_J(T) = I_{DS}^2 R \tau_{e-ph}$ ; here we take  $I_{DS} = 0.5$  mA and  $R = 4.4$  k $\Omega$ . Setting  $U_{ph} = U_J$  at the melting point we obtain  $\tau_{e-ph}(1680 \text{ K}) \approx 0.7 \times 10^{-7}$  s for our sample.

We can compare this value with an approximation for the bulk value. The electron–phonon relaxation time is related to the material resistivity  $\rho$ , the effective mass  $m^*$  and the carrier concentration  $n$  by

$$\tau_{e-ph} = \frac{m^*}{ne^2\rho}, \quad (1)$$

with  $e$  the electron charge [25]. We take  $\rho \approx 7.8 \times 10^{-3}$   $\Omega$  cm [27],  $m^* = 0.19m_0$  and  $n = 5 \times 10^{19}$  cm<sup>-3</sup> and we obtain  $\tau_{e-ph} \approx 2 \times 10^{-15}$  s as the approximated electron–phonon relaxation time at a temperature of about 1670 K in a bulk silicon sample with the same n-doping level as the measured nanostructure. This is a clear indication that the phonon density of states of the suspended nano-crystals is strongly reduced.

Using  $\tau_{e-ph} \approx 10^{-7}$  s we can in turn estimate the wire temperature at  $V_{DS} = 1$  V in figure 3(a) to be about 600 K. In this temperature regime the phonon energy is close to the boundary of the Brillouin zone, and relaxation occurs via Brillouin zone edge phonons [23]. The measured modulation of the conductance at large  $V_{DS}$  therefore directly reflects the phonon density of states. A variation of the bath temperature of the VTI up to 90 K has no significant influence as shown in the lower right inset of figure 3(a), in agreement with the assumption that the  $IV$  characteristic is at a wire temperature of about 600 K.

### 3. Conclusion

In summary, we have investigated the electronic properties of highly phosphorus-doped suspended silicon nanowires.

We found single-electron effects due to the random dopant distribution with a charging energy of the MTJs of about 4 meV. Furthermore, a strong conductance modulation at high drain–source currents is observed, which is interpreted as a direct fingerprint of electron relaxation via phonon emission. Finally, we find that due to the reduced electron scattering the nanowires can sustain extremely high current densities, which are of importance for hot-electron devices.

### Acknowledgment

We would like to thank J P Kotthaus and M L Roukes for detailed discussions. We acknowledge financial support from the Bundesministerium für Forschung und Technologie (BMBF 01M2413C6) and the Deutsche Forschungsgemeinschaft (Bl/487-2).

### References

- [1] Landauer R 1961 *IBM J. Res. Dev.* **5** 183
- [2] Kaganov M I, Lifshitz I M and Tanatarov L V 1957 *Sov. Phys.–JETP* **4** 173
- [3] Fujisawa T, Oosterkamp T H, van der Wiel W G, Broer B W, Aguado R, Tarucha S and Kouwenhoven L P 1998 *Science* **282** 932
- [4] Qin H, Holleitner A W, Eberl K and Blick R H 2001 *Phys. Rev. B* **64** R241302
- [5] Brandes T and Kramer B 1999 *Phys. Rev. Lett.* **83** 3021
- [6] Potts A *et al* 1991 *Superlatt. Microstruct.* **9** 315
- [7] Tighe T S, Worlock J M and Roukes M L 1997 *Appl. Phys. Lett.* **70** 2687
- [8] Beck R G, Eriksson M A, Westervelt R M, Campman K L and Gossard A C 1996 *Appl. Phys. Lett.* **68** 3763
- [9] Blick R H, Monzon F G, Wegscheider W, Bichler M, Stern F and Roukes M L 2000 *Phys. Rev. B* **62** 17 103
- [10] Fujii H, Kanemaru S, Matsukawa T and Itoh J 1999 *Appl. Phys. Lett.* **75** 3986
- [11] Pescini L, Tilke A, Blick R H, Lorenz H, Kotthaus J P, Eberhardt W and Kern D 1999 *Nanotechnology* **10** 418
- [12] Schwab K, Henriksen E A, Worlock J M and Roukes M L 2000 *Nature* **404** 974
- [13] Rego L G C and Kirczenow G 1998 *Phys. Rev. Lett.* **81** 232
- [14] DiTusa J F, Lin K, Park M, Isaacson M S and Parpia J M 1992 *Phys. Rev. Lett.* **68** 1156
- [15] Seyler J and Wybourne M N 1992 *Phys. Rev. Lett.* **69** 1427
- [16] Kanskar M and Wybourne M N 1994 *Phys. Rev. B* **50** 168
- [17] Smith R A and Ahmed H 1997 *J. Appl. Phys.* **81** 2699
- [18] Tilke A, Blick R H, Lorenz H, Kotthaus J P and Wharam D A 1999 *Appl. Phys. Lett.* **75** 3904
- [19] Pekola J P, Kauppinen J P and Paalanen M A 1994 *Phys. Rev. Lett.* **73** 2903
- [20] Tilke A T, Simmel F C, Blick R H, Lorenz H and Kotthaus J P 2001 *Prog. Quantum Electron.* **25/3** 97
- [21] Beenakker C W J 1991 *Phys. Rev. B* **44** 1646
- [22] Pekola J P, Taskinen L J and Farhangfar Sh 2000 *Appl. Phys. Lett.* **76** 3747
- [23] Yao Zh, Kane C L and Dekker C 2000 *Phys. Rev. Lett.* **84** 2941
- [24] Mermin D 1968 *Phys. Rev.* **176** 250
- [25] Kittel C 1996 *Introduction to Solid State Physics* 7th edn (New York: Wiley)
- [26] Shvartsburg A A and Jarrold M F 2000 *Phys. Rev. Lett.* **85** 2530
- [27] Pawlik M 1988 *Properties of Silicon* (INSPEC) p 83
- [28] French P J and Evans A G R 1988 *Properties of Silicon* (INSPEC) p 97